HHS Public Access

Author manuscript

Acta Biomater. Author manuscript; available in PMC 2020 January 15.

Published in final edited form as:

Acta Biomater. 2019 January 15; 84: 77–87. doi:10.1016/j.actbio.2018.11.035.

Blood Coagulation Response and Bacterial Adhesion to Biomimetic Polyurethane Biomaterials Prepared with Surface Texturing and Nitric Oxide Release

Li-Chong Xu[a,*], **Mark E. Meyerhoff**[b], and **Christopher A. Siedlecki**[a,c]

[a]Departments of Surgery, The Pennsylvania State University, College of Medicine, Hershey, PA 17033

[b]Department of Chemistry, University of Michigan, Ann Arbor, MI 48109

[c]Departments of Bioengineering, The Pennsylvania State University, College of Medicine, Hershey, PA 17033

Abstract

A dual functional polyurethane (PU) film that mimics aspects of blood vessel inner surfaces by combining surface texturing and nitric oxide (NO) release was fabricated through a soft lithography two-stage replication process. The fabrication of submicron textures on the polymer surface was followed by solvent impregnation with the NO donor, S-nitroso-N-acetylpenicillamine (SNAP). An *in vitro* plasma coagulation assay showed that the biomimetic surface significantly increased the plasma coagulation time and also exhibited reduced platelet adhesion and activation, thereby reducing the risk of blood coagulation and thrombosis. A contact activation assay for coagulation factor XII (FXII) demonstrated that both NO release and surface texturing also reduced FXII contact activation, which contributes to the inhibition of plasma coagulation. The biomimetic surface was also evaluated for bacterial adhesion in plasma and results demonstrate that this combined strategy enables a synergistic effect to reduce bacterial adhesion of *Staphylococcus epidermidis, Staphylococcus aureus,* and *Pseudomonas aeruginosa* microorganisms. The results strongly suggest that the biomimetic modification with surface texturing and NO release provides an effective approach to improve the biocompatibility of polymeric materials in combating thrombosis and microbial infection.

Keywords

Biomimetic; Surface Texturing; Nitric Oxide Release; Anticoagulation; Antibacteria

[*]Correspondence: The Pennsylvania State University, College of Medicine, Mail code H151, 500 University Drive Hershey, PA 17033. Phone: (717) 531-6130. Fax: (717) 531-4464. lxx5@psu.edu (Li-Chong Xu).

Author Contributions

Li-Chong Xu performed the experiments, analyzed the data, and drafted the manuscript. Mark Meyerhoff developed SNAP impregnation approach for creating thromboresistant and antimicrobial IV catheters and edited manuscript. Christopher Siedlecki provided guidance on experiments, assisted with analysis and discussion of data and edited manuscript.

Conflict of interest

The authors have no conflict of interest to disclose.

1. Introduction

Catheter-associated bloodstream infections are a major cause of death for hospitalized patients.[1] Intravascular catheters also increase the risk of thrombosis which has associated complications including endovascular infection, which further increases the risk of sequelae and requires prolonged antibiotic treatment.[2] Such biomaterial associated thrombosis and microbial infection have been barriers for implementation of the medical devices including catheters, stents, valves, ventricular assist devices in cardiovascular-healthcare. The development of new biomaterials possessing multifunctional surfaces that are anti-thrombotic, anti-microbial, and have improved tissue compatibility is critically important for the application of biomaterials as implants. Increasing amounts of data have shown that biomimetic strategies are effective approaches to control the biological responses toward foreign surfaces, thereby improving the biocompatibility of biomaterials.[3–6] One of the most attractive and interesting advantages is that these biomimetic approaches do not require incorporating antibiotics into materials that might lead to antibiotic resistant bacteria.

Biological responses to biomaterials are strongly surface property dependent. One promising approach to control biological responses is the generation of functional surfaces through biomimetic surface modification. Such surfaces significantly reduce the initial attachment of formed elements and organisms, including platelets and bacteria, to the surfaces of the implants. By mimicking natural antifouling surfaces such as shark skin, shell, or lotus leaf, the topographic surface modification of biomaterials with micro-or nano-structures can be an effective approach to reduce bacterial adhesion and inhibit biofilm formation[7–10] as well as to reduce platelet adhesion/activation.[11, 12] The mechanisms behind the prevention of biofilms and platelet adhesion by micro-or nano-topographic features are still not completely clear. However, the reduction of the surface effective contact area and the change in surface energy are believed to contribute to the antifouling properties of the surface.[13] For example, topographic surface modifications lower the surface energy that stabilizes a non-wetted state (i.e., superhydrophobicity) and prevents blood-material interactions, forming a blood-repellent superhydrophobic surface.[14] A variety of polymeric materials such as polypropylene,[15] poly(carbonate urethane),[16] polydimethylsiloxane (PDMS)[17] prepared via surface modification with micro-or nanostructured patterns have been reported to successfully reduce platelet binding and activation, thereby enhancing the blood compatibility. These superhydrophobic surfaces also reduce bacterial adhesion and biofilm formation, thereby decreasing microbial infection on the implants. Many of the approaches employing superhydrophobic materials for the reduction of bacterial adhesion have been reviewed elsewhere.[18] Previously we have developed submicron textured polyurethane (PU) biomaterial surfaces consisting of ordered arrays of pillars with dimension of 400/400 (diameter/spacing) nm and 500/500 nm, and demonstrated that these submicron textured surfaces significantly reduced bacterial adhesion, including for *Staphylococcal epidermidis* and *Staphylococcal aureus,* and inhibited biofilm formation under both shear and static conditions.[19] These previous works have also shown such submicron textured surfaces reduced platelet adhesion under shear.[20] These *in vitro* successes of materials with surface topographic modification have

demonstrated potential in combating microbial infections and thrombosis on biomedical devices and the great use in clinical applications.

Numerous studies have led to significant advancements towards the generation of biomaterials with improved hemocompatibility through a sole surface topographical design.[21, 22] However, the presence of small number of surface defects following fabrication may lead to local adhesion and accumulation of platelets or bacteria and has been a challenge for physical surface modification. Moreover, surface chemistry is often neglected when focusing on physical design of surface. In fact, chemical approaches have been widely applied in medical applications and are an important traditional surface modification technology [23, 24]. Thus, a combination of surface topography and surface chemistry may provide additional benefits, especially in eliminating any effects caused by physical defects in topographical modification. For instance, we developed polyethylene-glycol(PEG)-textured polyurethane biomaterials and results showed that the PEG-grafted submicron textured surface was more efficient in preventing biomaterial-associated thrombosis and infection of biomaterials than a single modification by either chemical or physical method alone, although there were difficulties with pillar collapse on these surfaces.[25]

The inner surface of a blood vessel is the best material for blood compatibility. Indeed, the inner surface of the aortic intima is not flat or smooth, but rather it is rough over the scale of several microns, with micro-grooves in the blood flow direction and nano-protuberances on the ridges.[26] At the same time, endothelial cells on the blood vessel surface produce nitric oxide (NO) which is known to contribute to anti-platelet activation/aggregation, anti-inflammation, and antibacterial properties of blood vessels in the cardiovascular system.[27, 28] NO release is a chemical modification approach with great potential for clinical use. Undoubtedly, the biocompatibility of blood vessels can be attributed to the unique multifunctionality and structured surfaces of vessel walls, and this provides a route to design new biomaterial surfaces with improvement of the biocompatibility of medical devices.

Toward this goal, we recently created a dual functional surface with a combination of surface texturing and NO release integrated on PU biomaterials, where *S*-nitroso-*N*-acetylpenicillamine (SNAP) was used as the NO donor within the PU and the surface was textured with submicron pillar patterns (Scheme 1).[29, 30] Results showed that the combination of surface texturing and NO release synergistic or additively reduced bacterial adhesion and inhibited biofilm formation. Moreover, utilizing an impregnation of SNAP in the polymer led to NO release at a stable and long term NO release for up to 38 days for 15% SNAP load, far longer than the NO release lifetime using a SNAP-doped PU with same amount of SNAP load.[30] While bacterial adhesion and biofilm formation on these biomimetic surfaces prepared with both texturing and NO release have been studied, the blood coagulation responses to such dual functioning surfaces have not yet been characterized. Herein we studied plasma coagulation, platelet adhesion/activation and plasma protein adsorption on such surfaces to understand the blood compatibility of these biomaterials. In addition, bacterial adhesion to surfaces was also studied in the presence of plasma which is to better replicate biological conditions. The systematic study of these biological interactions at dual functioning surfaces may demonstrate the potential of such biomimetic materials in medical devices for clinical use in blood contacting applications.

2. Materials and Methods

2.1 Materials.

CarboSil® 20 80A silicone polycarbonate-urethane (PU, DSM Biomedical Inc. Berkeley, CA) was used as the base polymer for experiments. PU was supplied as solids and dissolved in N,N-dimethylacetamide (DMAc, Sigma-Aldrich, St. Louis, MO) at a concentration of 15 w/v% for preparing the PU films. A silicon wafer patterned with pillars having diameter (d), spacing (s), and height (h) (d/s/h) of 700/700/300 nm was fabricated by the Pennsylvania State University Nanofabrication Facility (University Park, PA) and used as the master pattern to prepare PDMS molds and the corresponding CarboSil PU textured films. S-nitroso-N-acetylpenicillamine (SNAP) was purchased from PharmaBlock (Hatfield, PA). Methanol (MeOH) and methyl ethyl ketone (MEK) were the products of Fisher Scientific (Hampton, NH). Human fibrinogen was purchased from Calbiochem (La Jolla, CA) and human fibronectin was from Sigma-Aldrich (St. Louis, MO). Human FXII and αFXIIa were obtained from obtained from Enzyme Research Laboratories (South Bend, IN). Phosphate buffered saline (PBS 0.01 M, pH 7.4, Sigma-Aldrich) was prepared with Millipore water (18.2 MΩ). *S. epidermidis* RP62A (ATCC 35984), *S. aureus* Newman (ATCC 25904), and *Pseudomonas aeruginosa (P. aeruginosa,* ATCC 27853) were obtained from American Type Culture Collection (ATCC) (Manassas, VA) and used for the bacterial adhesion assay. To avoid contamination, all culture media and containers for bacterial study were autoclaved at 121 °C for 20 min, and the PU films were sterilized by washing with 70% ethanol prior to experiments.

2.2 Preparation of biomimetic PU films with surface texturing and NO release.

The textured PU film surfaces with ordered arrays of pillars were prepared by a modified soft lithography two-stage replication molding technique and impregnated with SNAP as described previously.[30] Briefly, a PDMS mold was obtained by casting against the Si wafer with the pattern of 700/700/300 nm and cured at 65°C under vacuum for 6 hrs to provide a negative silicone mold. A CarboSil PU solution was then spin-coated onto the silicon mold to prepare the textured PU films. To obtain high efficiency of textured topography, the films were prepared by spin casting PU onto a silicon mold at 1200 rpm for 1 min to add one thin layer first, followed by degassing and curing overnight at room temperature under vacuum. Then, additional layers of PU were added separately by spin casting at 600 rpm for 1 min, followed by degassing and curing under vacuum, respectively, until reaching the desired thickness of ~700 μm. The final products were dried at 65°C under vacuum overnight. Smooth CarboSil PU films were also prepared by spin-casting against a smooth PDMS mold using the same method.

To impregnate SNAP into PU films, small disks of films (10 mm in diameter) were punched from both smooth and textured CarboSil films. The films were soaked in solution (70 % MEK and 30 % MeOH) containing different SNAP concentrations (35 and 65 mg/mL) to achieve 5 and 10 wt% SNAP loading in CarboSil PU films, respectively[31]. After 2 h of impregnation, the films were removed from the impregnation solution, quickly washed with methanol to remove any residual SNAP solution on the film surface, and allowed to dry in an ambient environment protected from light exposure. Impregnated SNAP PU films with 5

and 10% into PU films release NO slowly and stably for 9 and 19 days, respectively, with a flux rate > 0.5×10^{-10} mol cm^{-2} min^{-1}, which represents the lower end of the physiological NO flux level exhibited by endothelial cells. [30].

2.3 Plasma coagulation time assay.

Citrated human platelet-poor plasma (PPP) was obtained from the blood bank at the Pennsylvania State University Milton S. Hershey Medical Center by pooling 5 units of outdated human plasma (within 5 d of expiration). The PPP was centrifuged at 1500 g and 25 °C for 20 min to remove the platelets. The PPP supernatant was then aliquoted in 15-mL polypropylene tubes (VWR) and stored at −20 °C. Prior to use, plasma were thawed for ~20 min in a 37 °C water bath.

The plasma coagulation response to biomaterials was measured by an *in vitro* coagulation time (CT) assay, which is defined as the time from activation of the blood coagulation cascade to the appearance of visible clot. The method is described in detail in previous publications.[32, 33] Briefly, a round piece of polymer film (~8 mm in diameter) was added to a 2 mL polystyrene tube containing 0.5 mL of human PPP. To this sample was then added 400 μL of PBS and 100 μL of 0.1 M $CaCl_2$ to start the coagulation process. The tube was immediately capped with parafilm and rotated at 8 rpm on a hematology mixer. The time from activation of the coagulation cascade (at point of addition of Ca^{2+}) to the first appearance of a visible clot was designated as the CT.

2.4 Human factor XII (FXII) contact activation assay.

Human FXII contact activation on biomaterial surfaces was carried out in polypropylene micro-centrifuge tubes (1.5 mL, VWR) at physiological concentration (30 μg/mL) in PBS buffer by incubation of ~330 μL protein solutions with an 8 mm diameter polymer film at room temperature on a hematology mixer, rotating at 8 rpm for 60 min. The tube was then centrifuged at 2000 rpm for 30s to obtain a supernatant of FXII after contact activation. This supernatant was then aliquoted and 100 μL was added to the plasma for measurement of CT. Meanwhile, an activated FXII (αFXIIa) was used as a standard reference, so that CTs of plasma supplemented with a series of concentrations of αFXIIa were used to generate a linear calibration curve when scaled on a logarithmic concentration axis over the concentrations of αFXIIa. The apparent αFXIIa concentrations following FXII contact activation with polymer films were obtained from this calibration curve.[34]

2.5 Assessment of platelet adhesion and activation on polymer surfaces.

Fresh human platelets were used for platelet adhesion experiments. Whole blood was drawn from the healthy human donors and collected in Vacutainer® plastic EDTA tubes (Becton Dickinson, Franklin Lakes, NJ) at The Pennsylvania State University Milton S. Hershey Medical Center. The protocol was approved by the Institutional Review Board. Blood was centrifuged at 180 g and 25 °C for 20 min to obtain platelet-rich plasma (PRP). The remaining blood was further centrifuged at 1500 g for 20 min to collect PPP. The concentration of platelets was determined by a Sysmex 9600 (Sysmex, Kobe, Japan) and adjusted to a concentration of 2.5×10^8 platelets/mL and using PPP for all platelet adhesion experiments.

A custom-made multi-well plate with volume of ~ 0.5 mL each well was used for platelet adhesion experiments as described previously.[35] Briefly, polymer films were cut into pieces with a diameter of 10 mm and mounted in the plate. Prior to the adhesion experiment, the films were pre-hydrated in Millipore water overnight, and were conditioned in PBS for 1 h to fully equilibrate the outermost surface of the polymer. Then PRP solution was added to replace the PBS in wells and incubated with polymer films at 37°C for 1 h under static condition. After incubation, samples were rinsed with PBS 3 times and fixed with 1% paraformaldehyde (PFA) for 1 h, followed by rinsing with PBS 3 times. The mouse anti-human $\alpha_{II}\beta_3$ antibody (ab662; Abcam Inc.) was used as the primary antibody to label all platelets adherent on the polymer film samples, using a dilution of 1.0 μL antibody in 1.5 mL of 6% normal serum (Jackson Immuno-Research Lab, Inc.). This primary antibody solution was incubated with samples overnight at 4°C. After removal of the primary antibody solution, samples were rinsed with PBS 3 times and then incubated with a secondary antibody solution (10 μL of AlexaFluor555 goat anti-mouse antibody IgG (Invitrogen) in 1 mL of 6% normal goat serum) in the dark at room temperature for 1 h. After rinsing, samples were mounted on a glass slide with a coverslip and antifade gel (Biomeda) and stored in a refrigerator overnight. The platelet adhesion samples were imaged at random locations on the surfaces using a fluorescent microscopy (Eclipse 80i, Nikon). The images were analyzed by Image J software to count the platelets per unit area.

To analyze the platelet activation adhered on the surfaces, the circularity of platelet morphology was further analyzed by Image J software. Circularity is defined by the formula: $circularity = \frac{4\pi\ area}{perimeter^2}$.The circularity values vary over the range between 0 and 1, indicating the degree of platelet activation. A circularity value of near to 1.0 indicates platelet in a round shape, suggesting that platelets are non-activated. In contrast, a lower value of circularity indicates increasingly activated platelets.

2.6 Protein adhesion force measurement by atomic force microscopy (AFM).

Adhesion forces between protein and polymer surface were measured by AFM and used to assess the interactions of proteins with the polymer film surfaces. Three test proteins, human fibrinogen (Fg), fibronectin (Fn), and FXII, were covalently coupled to AFM silicon nitride probes with long-narrow triangular cantilevers (Veeco Instruments, Santa Barbara, CA, nominal k= 0.06 N/m), as described in our previous publication.[36] Briefly, the probes were rinsed with acetone and treated by glow discharge plasma for 30 min and then incubated in a 1% (v/v) solution of aminopropyltriethoxysilane (Gelest Inc, PA) in ethanol for 1 h to provide reactive amine groups on the probes. After rinsing with Millipore water, the probes were reacted with 10% glutaraldehyde solution for 1 h. The probes were again rinsed with Millipore water to remove all glutaraldehyde from the solution, and incubated in protein solution (20 μg/ml) for 1 h. After removal of protein solutions, probes were stored in PBS at 4°C until use within 2 days. Multiple probes (>3) were prepared at the same time to improve consistency between experiments.

A Multimode AFM equipped with a Nanoscope Ilia controller system (Veeco Instruments, Santa Barbara, CA) was used for all force measurements. Experiments were performed in PBS using a fluid cell at a scan rate of 1 Hz and a z ramp size of 1 μm. A relative deflection

threshold of 100 nm was set at the trigger mode so that the total loading force was ~ 6.0 nN. Force volume imaging mode was used to collect the force data and a 16×16 array of force curves were collected over a scan area of 20×20 μm^2, ensuring that no area was sampled multiple times. Each sample was examined at least three different locations. The maximum deflection of AFM probe cantilever during retraction was defined as the adhesion force of protein and surface.

2.7 Bacterial adhesion assay in plasma solution.

Gram-positive (*S. epidermidis* RP62A and *S. aureus* Newman) and Gram-negative (*P. aeruginosa)* were used to assay the bacterial adhesion in plasma on the various polymeric surfaces. Bacteria were cultured in tryptic soy broth at 37 °C for 24 h and collected by centrifugation at 1360g for 10 min. The bacteria were then re-suspended in PBS and the concentration of bacteria was diluted to a final concentration of 1×10^8 CFU/mL with 50% human plasma and PBS, as determined by turbidity measurements at 600 nm using a spectrophotometer. All CarboSil films were pre-hydrated in Millipore water for 24 h and conditioned in PBS for 1 h before testing. Bacterial adhesion studies were conducted by placing the CarboSil films in a 12-well custom made multi-well plate containing 0.5 mL of bacteria suspended solution at 37°C for 2 h under near static conditions. The adhesion of *P. aeruginosa* was performed for 1 h because large bacterial aggregates were observed on control sample surfaces after 2 h and it is difficult to enumerate those bacterial cells. After the experiment, the film was washed with PBS 3×, and then fixed in 2.5% glutaraldehyde for 2 h. The bacterial cells on the film surfaces were stained with Gram Stain Stabilized Iodine kit (VWR). The samples were analyzed under an optical microscope (Nikon, Eclipse 80i). Nine optical microscopy images (91 μm × 68 μm) at random locations on each sample were taken and the number of bacteria adhered on the surface was counted to obtain a mean ± standard deviation value.

2.8 Data analysis.

Minitab software (version 18) was used for statistical analysis. Means of experimental data were compared by a 2-sample t-test and the effect of multiple variables on platelet or bacterial adhesions were analyzed by two-way ANOVA. Data were expressed as the mean ± standard deviation and p values of < 0.05 were considered significant.

3. Results

3.1 Plasma coagulation and FXII contact activation on biomaterial surfaces.

The blood coagulation responses to the polymer films were assessed by the *in-vitro* plasma coagulation time assay. The coagulation times of plasma incubated with the various CarboSil PU films are illustrated in Figure 1. The average CT of plasma in contact with smooth PU films was 17.9±0.5 min. The textured film slightly increased the coagulation time but not significantly (18.9 ± 1.6 min, p-value = 0.288). Both are significantly shorter than that of plasma in contact with the NO releasing films (24.3±1.4 min, $p<0.05$) while the coagulation time of control plasma without polymer films was 24.9±0.8 min. The surface textured and NO releasing PU films have similar coagulation times as the NO releasing only

polymer films, suggesting that NO plays an important role in inhibition of plasma coagulation.

The intrinsic pathway of plasma coagulation is regarded to be initiated by the activation of coagulation factor XII (FXII) in contact with biomaterial surface. The study of FXII contact activation by a surface is therefore useful to reveal the plasma coagulation property of biomaterials. Figure 2 illustrates the amount of activated FXII ($FXII_a$) produced after FXII was incubated with polymer films for 60 min. Results show that the highest amount of proteolytic enzyme $FXII_a$ was generated on smooth PU films with a yield of 0.64±0.08 ng/mm^2 (all are based on nominal surface area), which was significantly higher than the yields of FXIIa produced by the textured PU films without SNAP loaded (0.48 ±0.10 ng/mm^2, p=0.004). The impregnation of SNAP (either 5% or 10% loaded) in polymers further decreased $FXII_a$ yields, to only about one third of the amount of $FXII_a$ produced on smooth PU film surfaces. The films with combination of NO release and surface texturing provided the lowest $FXII_a$ values (0.14±0.01 ng/mm^2, p<0.001 compared to smooth or textured PU surfaces), consistent with the plasma coagulation result (Figure 1).

3.2 Platelet adhesion and activation on polymer film surfaces.

The platelet adhesion on polymer surfaces was performed in plasma at 37°C for 1 h under static condition and results are shown in Figure 3A. The results demonstrate that the textured film without SNAP significantly reduced platelet adhesion, with a reduction of 58% compared to the smooth, unloaded polyurethane biomaterials (p<0.001). The NO releasing surfaces with either 5% or 10% SNAP loading also significantly reduced the platelet adhesion with a reduction rate of approximately 76%. The combination of surface texturing and NO release further reduced platelet adhesion. The textured film surfaces with a 10% SNAP load produced the lowest platelet adhesion, where ~89% of platelet adhesion was inhibited (Table 1). No significant difference in platelet adhesion were observed between 5% and 10% SNAP impregnated PU films, either smooth or textured, and is most likely due to the similar NO flux rates from these 2 materials. Our previous study demonstrated that SNAP impregnation technique allowed SNAP to be embedded in the bulk of the material in a crystalline form. The formation of crystal-polymer composite initiates stable and long-term NO release with similar NO flux rates for different contents of SNAP, but the films loaded with higher content of SNAP release NO for longer time.[30] Herein, 5% and 10% SNAP impregnated PU films both release NO at flux rates of ~1.2–1.6 $\times 10^{-10}$ mol cm^{-2} min^{-1}, but the lifetime of NO release lasted for 9 and 19 days, respectively. ANOVA analysis shows that the effect of combining surface texturing with NO release is significant on reduction of platelet adhesion, suggesting that the combination of surface texturing and NO release synergistically inhibit platelet adhesion and reduces the potential of thrombosis ($p < 0.001$).

Surface texturing and NO release also decreased platelet activation on biomaterial surfaces. We use the morphological change of platelets, which can be quantitatively inferred from platelet circularity, to define the degree of platelet activation. Figure 3B illustrates the mean circularity values of platelets adhered on various PU film surfaces. Representative optical images of platelets adherent on the surfaces are shown in Figures 3C and 3D. Although the

lower mean value of circularity was found on the 10% SNAP smooth surface compared to 5% SNAP smooth surface, the difference was not significant, again likely due to the similar NO flux rates. The slight increase in circularity value of platelets on textured surface (0% SNAP) suggests that the surface texturing decreased the activation of platelets. The more significant change of circularity value was found on the platelets adhered on the biomimetic surfaces with combination of surface texturing and NO release, which are generally larger than 0.85, compared to the value of 0.77 on smooth surfaces. These data strongly suggested that a combination of NO release and surface texturing significantly decreases the activation of platelets, again reducing the risk of thrombosis.

3.3 Adhesion forces between proteins and surfaces.

The adhesion of proteins to the biomaterial surface was demonstrated by the measurement of adhesion forces between protein-coated probes and the surfaces using an AFM technique. The smooth PU (0% SNAP) and SNAP impregnated (10%) PU films were examined to study the effect of NO release on protein interaction with the surfaces. Human plasma proteins (Fg, Fn, or FXII) were covalently immobilized on the AFM probe and brought near the material surfaces so that interactions could be measured. The typical saw-tooth shaped retraction force curves were generally observed during the probe separation from the surfaces, indicating multiple interactions between the immobilized proteins and PU (both with and without NO release). Figure 4A illustrates such representative retraction force curves between the Fg modified probe tip and the PU surfaces. However, the NO releasing surface (10% SNAP) exhibited lower adhesive forces compared to the PU surface without NO release. AFM force mapping was used to acquire the adhesion forces and the forces were extracted from force volume data and pooled together. Forces are presented as histograms showing the distributions of adhesion forces of proteins (see Figures 4b–4d). In all cases, the histogram of forces is shifted to the left for the NO releasing materials, indicating lower adhesion forces when NO release is present. The peak of the histogram of Fg with the PU surface appeared around 1.05 nN, while the peak for interactions of Fg and NO releasing PU surface was observed at 0.85 nN. The mean adhesion forces of Fg to surfaces were 1.08±0.16 nN and 0.81±0.21 nN for regular PU and NO releasing surfaces, respectively (Figure 5). Fn and FXII produced similar force histograms, but with smaller adhesion forces compared to the Fg. Statistical analysis showed that the NO releasing surfaces yielded significantly smaller adhesion forces than the regular PU surface for all three proteins ($p<0.001$, Figure 5). This suggests that NO release may influence the subsequent plasma coagulation, platelet adhesion, and bacterial adhesion.

3.4 Bacterial adhesion responses of textured and NO releasing PU surfaces.

Three of the most prevalent pathogens found in the setting of biomaterial-associated infections: *S. epidermidis, S. aureus,* and *P. aeruginosa,* were used to assess bacterial adhesion to the various PU films in plasma under static conditions (Figure 6). Generally, both the textured alone and the NO releasing alone materials significantly reduced bacterial adhesion in plasma ($p<0.001$). Compared to a single surface treatment (texturing or NO release alone), the combination of surface texturing and NO release further reduced the bacterial adhesion. For example, the surface texturing and NO release reduced *S. epidermidis* adhesion in plasma over a 2 h period approximately 56% and 76%, respectively,

but the combination of both modifications reduced bacterial adhesion by ~84% (Figure 6A and Table 2). Similar results were observed for the adhesion of *S. aureus* onto the various surfaces. The bacterial adhesion of *P. aeruginosa* on polymer surfaces was performed for only 1 h due to the very large aggregates of bacterial cells observed on control smooth PU surfaces after a 2 h period. In this case, the combination of surface texturing and SNAP impregnation significantly reduce bacterial adhesion up to approximately 87%. The two-way ANOVA statistical analysis show that the combination of surface texturing and NO release significantly reduced the bacterial adhesion (p values < 0.05 for all bacteria), suggesting that surface texturing and NO release synergistically decrease bacterial adhesion in plasma.

4. Discussion

Biocompatibility is the central tenant for the application of biomaterials in blood-contacting medical devices, but biomaterial induced thrombosis and infection have been problematic issues for the use of these devices. Both biological responses are largely dependent on the surface properties of biomaterials used to prepare the devices. Biomimetic surface modification approaches such as physical topographical modification[37, 38] and NO release[39, 40] to combat thrombosis and microbial infection are attractive and have developed substantially in recent years. The combination of surface texturing and NO release on PU biomaterials produces a biomimetic and multifunctional surface based on what is present on the inner surface of blood vessels and has demonstrated efficiency in controlling bacterial adhesion and biofilm formation, thereby potentially reducing microbial infection.[29, 30] The surface properties of these materials, including surface chemistry, physicochemical properties, NO release flux, and bacterial and biofilm responses have been extensively studied in our previous research. This work focuses on blood coagulation responses and new bacterial adhesion responses in plasma to the surface textured and NO releasing polyurethane films.

Blood coagulation induced by biomaterials is due to plasma coagulation itself but also mediated by platelet reactions. Plasma coagulation due to contact with biomaterials occurs through the intrinsic pathway of the blood coagulation cascade, which is initiated by contact activation of FXII conversion to proteolytic enzyme FXIIa. $FXII_a$ in turn triggers a series of zymogen to enzyme conversions that eventually leads to the generation of thrombin.[41] Interactions of platelets and biomaterials include the adhesion, activation, and aggregation of platelets on material surfaces. Therefore, analysis of plasma coagulation, FXII contact activation, and platelet adhesion and activation are all direct approaches to evaluate the blood coagulation responses to implanted biomaterials.

4.1 NO inhibits plasma coagulation through the inhibition of FXII contact activation.

While numerous studies have shown the inhibition of platelet activation and aggregation by NO, the effect of NO on plasma coagulation (without platelets involved) was unexpected. The coagulation time assay demonstrated that the NO-donor impregnated polymers significantly increased the coagulation time of plasma compared to either smooth or textured polymers without the NO-donor (0% SNAP, $p<0.05$, Figure 1). However, the difference in coagulation time between NO-donor impregnated polymers and control plasma (without

polymer contact) was not significant ($p>0.05$). The experimental results also showed that the surface texturing slightly increases plasma coagulation time, but again, non-significantly. Both results suggest that NO release plays an important role in the inhibition of plasma coagulation. As the biomaterial associated plasma coagulation is known to be initiated by FXII contact activation of the intrinsic pathway of the blood coagulation cascade, this study further demonstrates that SNAP impregnated polymer surface and/or NO release inhibited the initial FXII contact activation (Figure 2), that may explain the inhibition of plasma coagulation by NO.

FXII contact activation is surface dependent and influenced by surface wettability, surface charge, and surface chemistry.[42] The results in this study suggest that the SNAP impregnation may influence the surface properties such as surface chemistry and surface charge, thereby inhibiting FXII contact activation. Furthermore, and perhaps more importantly, NO free radicals which are released from the polymer may also represent an additional regulatory mechanism for the formation of blood clot through inhibition of FXII contact activation. Catani *et al.* reported that NO can inhibit blood coagulation factor XIII (FXIII), the last enzyme of the coagulation cascade, through *S*-nitrosylation of a crucial titratable cysteine residue.[43] This study, for the first time, demonstrates that NO potentially inhibits the FXII contact activation, the first enzyme of the blood coagulation cascade, and this underlying effect on contact activation should be further studied in future.

4.2 Surface texturing and NO release synergistically inhibits platelet adhesion and activation.

NO is an endogenous gas molecule and plays an important protective role in the cardiovascular system. NO acts as a signaling molecule and inhibits platelet activation and aggregation on the inner surface of blood vessel walls through the soluble guanylate cyclase (sGC) that converts guanosine triphosphate (GTP) to cyclic guanosine monophosphate (cGMP). [44–46] The cGMP also activates the cGMP-dependent protein kinases (cGKs) and increases cyclic adenosine monophosphate (cAMP) that activates the cAMP-dependent protein kinase (PKA), a known platelet inhibitor.[47] The NO-induced sGC ultimately results in reduced intracellular calcium, inhibition of platelet phosphoinositide 3-kinase, and reduces affinity as well as number of surface membrane fibrinogen binding sites on the surface of platelets (GPIIb/IIIa)[39]. Therefore, NO releasing materials represent a very promising approach to prevent thrombus associated complications in blood contacting medical devices. Over the past two decades, many researchers have developed NO releasing polymers and studied the properties of platelet inhibition *in-vitro* and *in-vivo.* Mowery *et al.* developed PVC-or PU-based polymer films containing an NO releasing diazeniumdiolate *via* different approaches such as dispersion, covalent bounding or ion-pairing of NO donors and demonstrated significant improvements in blood compatibility through *in vitro* platelet adhesion tests.[48] Brisbois *et al.* developed SNAP-doped Elast-eon E2As polymers with long-term NO release and elevated temperature stability, and found that platelet counts in extracorporeal blood flow were preserved at 100±7% of baseline for the SNAP/E2As coated loops, compared to 60 ± 6% for E2As control circuits, suggesting the SNAP/E2As coating has potential to improve the thromboresistance of not only extracorporeal circuits but also intravascular catheters, grafts, and other blood-contacting medical devices. [49] The platelet

adhesion on NO releasing polymer surfaces appears to correlate with NO flux levels. Wu *et al.* found that fewer platelets were adhered on the polymer films impregnated with higher concentrations of NO donor and with higher NO flux level.[50] It should be noted that the SNAP impregnated PU films employed in this study containing 5% and 10% SNAP content released NO at a flux in the range of $(1.0 – 2.0)\times10^{-10}$ mol $min^{-1}cm'^{2}$ but with different life-times of NO release (9 d vs. 19 d).[30] Thus, it is not surprising that the platelet adhesion was similar on both smooth film surfaces, but significantly lower than the control PU films (Figure 3A). Contrasting the NO release approach, the mechanism of platelet inhibition by micro-structured surfaces is not fully understood. Milner *et al.* found that the surface textures with sub-platelet dimensions may reduce platelet adhesion from plasma onto the material surface, suggesting the reduction of accessible surface contact area may contribute to low adhesion of platelets and also lower activation of platelets.[20] In addition, the change of surface wettability due to surface texturing may be another reason for lower platelet adhesion and activation.[51] This new study shows that the combination of surface texturing and NO release further significantly and synergistically inhibited platelet adhesion (Figure 3), suggesting that the combination of physical surface modification and chemical functional treatment can dramatically increase the efficiency in the inhibition of platelet adhesion, thereby reducing the potential for thrombosis.

4.3 NO release reduces plasma protein adhesion and influences blood coagulation and bacterial adhesion responses to surfaces.

Protein adsorption is the first event during the interaction of blood with implanted biomaterials and influences the subsequent biological responses including platelet and bacterial adhesion. Fibrinogen and fibronectin are the most important proteins influencing platelet adhesion/activation[52] and bacterial adhesion[53] while FXII is the initial protein involved in the contact activation complex of the intrinsic pathway of the blood coagulation cascade.[42] This study demonstrated that the adhesion forces of these three proteins were all smaller when interacting with NO releasing surfaces than with the regular PU surfaces (Figures 4 and 5), indicating that NO releasing surfaces appear to reduce the binding/adsorption of proteins with surfaces, which may induce lower platelet adhesion and bacterial adhesion. The reduced binding of FXII may also decrease the contact activation of FXII. However, the adsorption of proteins on NO releasing surfaces appears complicated and a function of the NO flux. It was found previously that an NO releasing material with a surface NO flux of $17.4 \pm 0.5\times10^{-10}$ mol cm^{-2} min^{-1}, significantly higher than the NO flux in this study ($1.6\pm0.2 \times10^{-10}$ mol cm^{-2} min^{-1}), showed a significant *increase* in the amount of fibrinogen adsorbed to the material surface compared to one with a low flux of NO and the control.[54] This may trigger more interest to study in more detail the effects of NO release rate on protein adsorption and activity using NO releasing surface, which are beyond the scope of this study.

4.4 Surface texturing and NO release synergistically inhibit the bacterial adhesion in plasma.

As a diatomic free radical, NO exerts broad-spectrum antimicrobial activity against pathogens and reduces health care-associated infections through inhibition of bacterial respiration, DNA replication or specific metabolic pathways, such as the tricarboxylic acid

cycle.[55] It has been clearly demonstrated in recent years that NO releasing/generating polymers can have strong antibacterial effects and effectively reduce bacterial adhesion and inhibit biofilm development on material surfaces.[56–58] Physical topographical surface modifications such as texturing reduces the available surface contact area for bacterial interactions and changes the surface wettability, thereby inhibiting bacterial adhesion or more easily disrupting biofilm formation.[13, 19] As expected, and as shown here, the combination of surface topographical modification and NO release enhances the reductions in bacterial adhesion and biofilm formation. In a previous study, we demonstrated the antibacterial activity of surface textured and SNAP impregnated PU films against *S. epidermidis, S. aureus, P. aeruginosa,* and *E. coli,* and results showed that the combination of surface texturing and NO release could synergistically or additively inhibit bacterial adhesion to surfaces in PBS solution. [30] Long-term biofilm studies showed that the dual functioning PU surfaces with texturing and NO release inhibit biofilm formation for at least 28 days.[29] The study in this manuscript further measured the bacterial adhesion on surfaces in plasma solutions where the plasma proteins may adsorb on surfaces and influence bacterial adhesion, and results again showed that surface texturing and NO release can synergistically reduce bacterial adhesion in plasma solutions for *S. epidermidis, S. aureus,* and *P. aeruginosa* (Figure 6, Table 2). The antibiofilm properties of such dual functional surfaces have also been evaluated in previous study.[30] It can be concluded that the combination of surface texturing and NO release can either synergistically or additively inhibit bacterial adhesion both in PBS and plasma solutions (this study), and reduces biofilm formation. This provides a potential for use in combatting the occurrence of microbial infections on medical devices.

Biomimetic surface modification with combination of surface texturing and NO release exhibits significant inhibition of FXII contact activation, platelet adhesion/activation, and bacterial adhesion, thereby providing the great potential for reducing the risks of thrombosis and microbial infection. Colletta *et al.* [59] used a mouse fibroblast cell-line model and found that the SNAP-impregnated catheters were fully biocompatible as extracts of the catheter tubing scored 0 for in vitro toxicity testing (0–1=safe, 3–4=toxic). The Handa group recently developed a SNAP covalently immobilized PDMS films and found more than 96% of mouse fibroblast cells were viable when exposed to the leachates from SNAP-PDMS films for 24 h.[60] In another work on the liquid-infused nitric oxide-releasing material by incorporated with SNAP, the leachates from materials not only did not cause any cytotoxic responses, but at the same time they promoted the proliferation of the mouse fibroblast cells. [61] All these works suggest that the leachates from SNAP-incorporated materials are non-toxic to cells.

SNAP-impregnated PU biomaterials exhibit long-term NO release. NO release from SNAP varies with temperature, pH, and surrounding environment. The half-life of SNAP is only approximately six hours in the presence of transition metal ion chelators[62]. However, the release of physiologic levels of NO from 5%, 10%, and 15% SNAP impregnated PU films extends to 9, 19, and 38 days, respectively, under 37°C in PBS in the absence of transition metal ions[30], suggesting SNAP is more stable when placed in polymers via impregnation. Future work will include efforts to explore the impregnation technique or other techniques to incorporate SNAP into polymers for increasing lifetime of NO release. However, the

addition of surface texturing to the NO releasing system will help to increase the protection time from platelet/bacteria adhesion because surface texturing will keep functioning for resistance to blood coagulation and biofilm formation after NO release is exhausted. Taken together, we can conclude that the combination of surface texturing and NO release appears to provide a safe approach to dramatically reduce the risks of thrombosis and infection, and significantly improve the biocompatibility of biomaterials. Future steps in this work will include long term animal testing to ensure that these benchtop results translate to *in-vivo*.

5. Conclusion

A dual functional polyurethane polymer film with combined surface texturing and NO release was prepared by fabricating polymeric films bearing ordered submicron pillars on the surface, and then subsequently solvent impregnating the films with the NO donor SNAP. This approach significantly inhibits plasma coagulation and increases the plasma coagulation time through the reduction of contact activation of FXII by NO release. Biomimetic modification of biomaterials with surface texturing and NO release synergistically reduced the platelet adhesion and activation, and bacterial adhesion in plasma. Results suggested that biomimetic modification provides an effective approach to improve the biocompatibility of biomaterials/polymers used to prepare blood contacting medical devices.

Acknowledgements

Research reported in this publication was supported by the National Institute of Allergy and Infectious Disease of NIH under award number R21AI139706. In addition, MEM acknowledges NIH grant RO1 HL128337–01 for supporting the SNAP impregnation approach for creating thromboresistant and antimicrobial IV catheters.

7. References

[1]. Wenzel RP, Edmond MB, The impact of hospital-acquired bloodstream infections, Emerging Infectious Diseases 7(2) (2001) 174–177. [PubMed: 11294700]

[2]. Rooden C.J.v., Schippers EF, Barge RMY, Rosendaal FR, Guiot HFL, Meer F.J.M.v.d., Meinders AE, Huisman MV, Infectious Complications of Central Venous Catheters Increase the Risk of Catheter-Related Thrombosis in Hematology Patients: A Prospective Study, Journal of Clinical Oncology 23(12)(2005)2655–2660. [PubMed: 15837979]

[3]. Damodaran VB, Murthy NS, Bio-inspired strategies for designing antifouling biomaterials, Biomaterials Research 20(1) (2016) 18. [PubMed: 27326371]

[4]. Tsiapalis D, De Pieri A, Biggs M, Pandit A, Zeugolis DI, Biomimetic Bioactive Biomaterials: The Next Generation of Implantable Devices, ACS Biomaterials Science & Engineering 3(7) (2017) 1172–1174.

[5]. Rahmany MB, Van Dyke M, Biomimetic approaches to modulate cellular adhesion in biomaterials: A review, Acta Biomaterialia 9(3) (2013) 5431–5437. [PubMed: 23178862]

[6]. Weng Y, Chen J, Tu Q, Li Q, Maitz MF, Huang N, Biomimetic modification of metallic cardiovascular biomaterials: from function mimicking to endothelialization in vivo, Interface Focus (2012).

[7]. Scardino AJ, Hudleston D, Peng Z, Paul NA, de Nys R, Biomimetic characterisation of key surface parameters for the development of fouling resistant materials, Biofouling 25(1) (2009) 83–93. [PubMed: 18985468]

[8]. Scardino AJ, Zhang H, Cookson DJ, Lamb RN, de Nys R, The role of nano-roughness in antifouling, Biofouling 25(8) (2009) 757–767. [PubMed: 20183134]

[9]. Barthlott W, Neinhuis C, Purity of the sacred lotus, or escape from contamination in biological surfaces, Planta 202(1) (1997) 1–8.

[10]. Bhushan B, Jung YC, Natural and biomimetic artificial surfaces for superhydrophobicity, self-cleaning, low adhesion, and drag reduction, Progress in Materials Science 56(1) (2011) 1–108.

[11]. Moradi S, Hadjesfandiari N, Toosi SF, Kizhakkedathu JN, Hatzikiriakos SG, Effect of Extreme Wettability on Platelet Adhesion on Metallic Implants: From Superhydrophilicity to Superhydrophobicity, ACS Applied Materials & Interfaces 8(27) (2016) 17631–17641. [PubMed: 27322889]

[12]. Park JY, Gemmell CH, Davies JE, Platelet interactions with titanium: modulation of platelet activity by surface topography, Biomaterials 22(19) (2001) 2671–2682. [PubMed: 11519787]

[13]. Xu LC, Siedlecki CA, Staphylococcus epidermidis adhesion on hydrophobic and hydrophilic textured biomaterial surfaces, Biomedical Materials 9(3) (2014) 035003.

[14]. Jokinen V, Kankuri E, Hoshian S, Franssila S, Ras RHA, Superhydrophobic Blood-Repellent Surfaces, Advanced Materials (2018) 1705104.

[15]. Hou XM, Wang XB, Zhu QS, Bao JC, Mao C, Jiang LC, Shen JA, Preparation of polypropylene superhydrophobic surface and its blood compatibility, Colloids and Surfaces B-Biointerfaces 80(2) (2010) 247–250.

[16]. Sun T, Tan H, Han D, Fu Q, Jiang L, No Platelet Can Adhere—Largely Improved Blood Compatibility on Nanostructured Superhydrophobic Surfaces, Small 1(10) (2005) 959–963. [PubMed: 17193377]

[17]. Zhou M, Yang JH, Ye X, Zheng AR, Li G, Yang PF, Zhu Y, Cai L, Blood platelet's behavior on nanostructured superhydrophobic surface, Journal of Nano Research, Trans Tech Publ, 2008, pp. 129–136.

[18]. Zhang X, Wang L, Levanen E, Superhydrophobic surfaces for the reduction of bacterial adhesion, RSC Advances 3(30) (2013) 12003–12020.

[19]. Xu L-C, Siedlecki CA, Submicron-textured biomaterial surface reduces staphylococcal bacterial adhesion and biofilm formation, Acta Biomaterialia 8(1) (2012) 72–81. [PubMed: 21884831]

[20]. Milner KR, Snyder AJ, Siedlecki CA, Sub-micron texturing for reducing platelet adhesion to polyurethane biomaterials, Journal of Biomedical Materials Research Part A 76A(3) (2006) 561–570.

[21]. Liu X, Yuan L, Li D, Tang Z, Wang Y, Chen G, Chen H, Brash JL, Blood compatible materials: state of the art, Journal of Materials Chemistry B 2(35) (2014) 5718–5738.

[22]. Chen L, Han D, Jiang L, On improving blood compatibility: From bioinspired to synthetic design and fabrication of biointerfacial topography at micro/nano scales, Colloids and Surfaces B: Biointerfaces 85(1) (2011) 2–7. [PubMed: 21106352]

[23]. Ikada Y, Surface modification of polymers for medical applications, Biomaterials 15(10) (1994) 725–736. [PubMed: 7986935]

[24]. Roach P, Eglin D, Rohde K, Perry CC, Modern biomaterials: a review-bulk properties and implications of surface modifications, Journal of Materials Science-Materials in Medicine 18(7) (2007) 1263–1277. [PubMed: 17443395]

[25]. Xu L-C, Siedlecki CA, Protein adsorption, platelet adhesion, and bacterial adhesion to polyethylene-glycol-textured polyurethane biomaterial surfaces, Journal of Biomedical Materials Research Part B: Applied Biomaterials 105(3) (2017) 668–678. [PubMed: 26669615]

[26]. Klee D, Hocker H, Polymers for biomedical applications: Improvement of the interface compatibility, Biomedical Applications: Polymer Blends1999, pp. 1–57.

[27]. Carpenter AW, Schoenfisch MH, Nitric oxide release: Part II. Therapeutic applications, Chemical Society Reviews 41(10) (2012) 3742–3752. [PubMed: 22362384]

[28]. Strijdom H, Chamane N, Lochner A, Nitric oxide in the cardiovascular system: a simple molecule with complex actions, Cardiovascular Journal of Africa 20(5) (2009) 303–310. [PubMed: 19907806]

[29]. Xu L-C, Wo Y, Meyerhoff ME, Siedlecki CA, Inhibition of bacterial adhesion and biofilm formation by dual functional textured and nitric oxide releasing surfaces, Acta Biomaterialia 51 (2017) 53–65. [PubMed: 28087484]

[30]. Wo Y, Xu LC, Li Z, Matzger AJ, Meyerhoff ME, Siedlecki CA, Antimicrobial nitric oxide releasing surfaces based on S-nitroso-N-acetylpenicillamine impregnated polymers combined with submicron-textured surface topography, Biomaterals Science 5(7) (2017) 1265–1278.

[31]. Wo Y, Brisbois EJ, Wu J, Li Z, Major TC, Mohammed A, Wang X, Colletta A, Bull JL, Matzger AJ, Xi C, Bartlett RH, Meyerhoff ME, Reduction of Thrombosis and Bacterial Infection via Controlled Nitric Oxide (NO) Release from S-Nitroso-N-acetylpenicillamine (SNAP) Impregnated CarboSil Intravascular Catheters, ACS Biomater Sci Eng 3(3) (2017) 349–359. [PubMed: 28317023]

[32]. Chatterjee K, Guo Z, Vogler EA, Siedlecki CA, Contributions of contact activation pathways of coagulation factor XII in plasma, J Biomed Mater Res A 90(1) (2009) 27–34. [PubMed: 18481791]

[33]. Chatterjee K, Thornton JL, Bauer JW, Vogler EA, Siedlecki CA, Moderation of prekallkrein-factor XII interactions in surface activation of coagulation by protein-adsorption competition, Biomaterials 30(28) (2009) 4915–4920. [PubMed: 19552950]

[34]. Guo Z, Bussard KM, Chatterjee K, Miller R, Vogler EA, Siedlecki CA, Mathematical modeling of material-induced blood plasma coagulation, Biomaterials 27(5) (2006) 796–806. [PubMed: 16099033]

[35]. Xu L-C, Li Z, Tian Z, Chen C, Allcock HR, Siedlecki CA, A new textured polyphosphazene biomaterial with improved blood coagulation and microbial infection responses, Acta Biomaterialia 67 (2018) 87–98. [PubMed: 29229544]

[36]. Xu LC, Siedlecki CA, Effects of surface wettability and contact time on protein adhesion to biomaterial surfaces, Biomaterials 28(22) (2007) 3273–3283. [PubMed: 17466368]

[37]. Harvey AG, Hill EW, Bayat A, Designing implant surface topography for improved biocompatibility, Expert Review of Medical Devices 10(2) (2013) 257–267. [PubMed: 23480094]

[38]. Jaggessar A, Shahali H, Mathew A, Yarlagadda PKDV, Bio-mimicking nano and micro-structured surface fabrication for antibacterial properties in medical implants, Journal of Nanobiotechnology 15(1) (2017) 64. [PubMed: 28969628]

[39]. Wo Y, Brisbois EJ, Bartlett RH, Meyerhoff ME, Recent advances in thromboresistant and antimicrobial polymers for biomedical applications: just say yes to nitric oxide (NO), Biomaterials Science 4(8) (2016) 1161–1183. [PubMed: 27226170]

[40]. Margel D, Mizrahi M, Regev-Shoshani G, Ko M, Moshe M, Ozalvo R, Shavit-Grievink L, Baniel J, Kedar D, Yossepowitch O, Lifshitz D, Nadu A, Greenberg D, Av-Gay Y, Nitric oxide charged catheters as a potential strategy for prevention of hospital acquired infections, Plos One 12(4) (2017) e0174443.

[41]. Colman RW, Scott CF, Schmaier AH, Wachtfogel YT, Pixley RA, Edmunds LH, Initiation of Blood Coagulation at Artificial Surfaces, Annals of the New York Academy of Sciences 516(1) (1987) 253–267. [PubMed: 3439730]

[42]. Vogler EA, Siedlecki CA, Contact activation of blood-plasma coagulation, Biomaterials 30(10) (2009) 1857–1869. [PubMed: 19168215]

[43]. Catani MV, Bernassola F, Rossi A, Melino G, Inhibition of Clotting Factor XIII Activity by Nitric Oxide, Biochemical and Biophysical Research Communications 249(1) (1998) 275–278. [PubMed: 9705871]

[44]. Lei J, Vodovotz Y, Tzeng E, Billiar TR, Nitric oxide, a protective molecule in the cardiovascular system, Nitric Oxide 35 (2013) 175–185. [PubMed: 24095696]

[45]. Radomski MW, Palmer RMJ, Moncada S, The role of nitric oxide and cGMP in platelet adhesion to vascular endothelium, Biochemical and Biophysical Research Communications 148(3) (1987) 1482–1489. [PubMed: 2825688]

[46]. Denninger JW, Marietta MA, Guanylate cyclase and the NO/cGMP signaling pathway, Biochimica et Biophysica Acta (BBA) -Bioenergetics 1411(2) (1999) 334–350. [PubMed: 10320667]

[47]. Du X, A new mechanism for nitric oxide– and cGMP-mediated platelet inhibition, Blood 109(2) (2007) 392–393.

[48]. Mowery KA, Schoenfisch MH, Saavedra JE, Keefer LK, Meyerhoff ME, Preparation and characterization of hydrophobic polymeric films that are thromboresistant via nitric oxide release, Biomaterials 21(1) (2000) 9–21. [PubMed: 10619674]

[49]. Brisbois EJ, Handa H, Major TC, Bartlett RH, Meyerhoff ME, Long-term nitric oxide release and elevated temperature stability with S-nitroso-N-acetylpenicillamine (SNAP)-doped Elast-eon E2As polymer, Biomaterials 34(28) (2013) 6957–66. [PubMed: 23777908]

[50]. Wu Y, Zhou Z, Meyerhoff ME, In vitro platelet adhesion on polymeric surfaces with varying fluxes of continuous nitric oxide release, Journal of Biomedical Materials Research Part A 81A(4) (2007) 956–963.

[51]. Ye X, Shao Y.-l., Zhou M, Li J, Cai L, Research on micro-structure and hemo-compatibility of the artificial heart valve surface, Applied Surface Science 255(13–14) (2009) 6686–6690.

[52]. Xu L-C, Soman P, Scheetz BM, Siedlecki CA, Measurement of time-dependent functional activity of adsorbed fibrinogen and platelet adhesion on material surfaces, in: Horbett T, Brash JL, Norde W (Eds.), Proteins at Interfaces Iii: State of the Art2012, pp. 373–394.

[53]. Xu LC, Siedlecki CA, Effects of Plasma Proteins on Staphylococcus epidermidis RP62A Adhesion and Interaction with Platelets on Polyurethane Biomaterial Surfaces, Journal of Biomaterials and Nanobiotechnology 3(4A) (2012) 487–498.

[54]. Lantvit SM, Barrett BJ, Reynolds MM, Nitric oxide releasing material adsorbs more fibrinogen, Journal of Biomedical Materials Research Part A 101(11) (2013) 3201–3210. [PubMed: 23554300]

[55]. Fang FC, Antimicrobial actions of nitric oxide, Nitric Oxide 27 (2012) S10.

[56]. Hetrick EM, Shin JH, Stasko NA, Johnson CB, Wespe DA, Holmuhamedov E, Schoenfisch MH, Bactericidal Efficacy of Nitric Oxide-Releasing Silica Nanoparticles, ACS Nano 2(2) (2008) 235–246. [PubMed: 19206623]

[57]. Singha P, Pant J, Goudie MJ, Workman CD, Handa H, Enhanced antibacterial efficacy of nitric oxide releasing thermoplastic polyurethanes with antifouling hydrophilic topcoats, Biomater Sci 3(10) (2017).

[58]. Mann MN, Neufeld BH, Hawker MJ, Pegalajar-Jurado A, Paricio LN, Reynolds MM, Fisher ER, Plasma-modified nitric oxide-releasing polymer films exhibit time-delayed 8-log reduction in growth of bacteria, Biointerphases 11(3) (2016) 4959105.

[59]. Colletta A, Wu J, Wo Y, Kappler M, Chen H, Xi C, Meyerhoff ME, S-Nitroso-N-acetylpenicillamine (SNAP) Impregnated Silicone Foley Catheters: A Potential Biomaterial/Device To Prevent Catheter-Associated Urinary Tract Infections, ACS Biomaterials Science & Engineering 1(6) (2015) 416–424. [PubMed: 26462294]

[60]. Hopkins SP, Pant J, Goudie MJ, Schmiedt C, Handa H, Achieving Long-Term Biocompatible Silicone via Covalently Immobilized S-Nitroso-N-acetylpenicillamine (SNAP) That Exhibits 4 Months of Sustained Nitric Oxide Release, ACS Applied Materials & Interfaces 10(32) (2018) 27316–27325. [PubMed: 30028941]

[61]. Goudie MJ, Pant J, Handa H, Liquid-infused nitric oxide-releasing (LINORel) silicone for decreased fouling, thrombosis, and infection of medical devices, Scientific Reports 7(1) (2017) 13623. [PubMed: 29051609]

[62]. Singh RJ, Hogg N, Joseph J, Kalyanaraman B, Mechanism of Nitric Oxide Release from S-Nitrosothiols, Journal of Biological Chemistry 271(31) (1996) 18596–18603. [PubMed: 8702510]

Statement of Significance

1. Developed a dual functional polyurethane (PU) film that mimics blood vessel inner surface by combining surface texturing and nitric oxide (NO) release for combatting biomaterial associated thrombosis and microbial infection.
2. Studied the blood coagulation response and bacterial adhesion to such biomimetic PU surfaces, and demonstrated that the combination of surface texturing and NO release synergistically reduced the platelet adhesion and bacterial adhesion in plasma, providing an effective approach to improve the biocompatibility of biomaterials used in blood-contacting medical devices.
3. The NO releasing surface significantly inhibits the plasma coagulation via the reduction of contact activation of FXII, indicating the multifunctional roles of NO in improving the biocompatibility of biomaterials in blood-contacting medical devices.

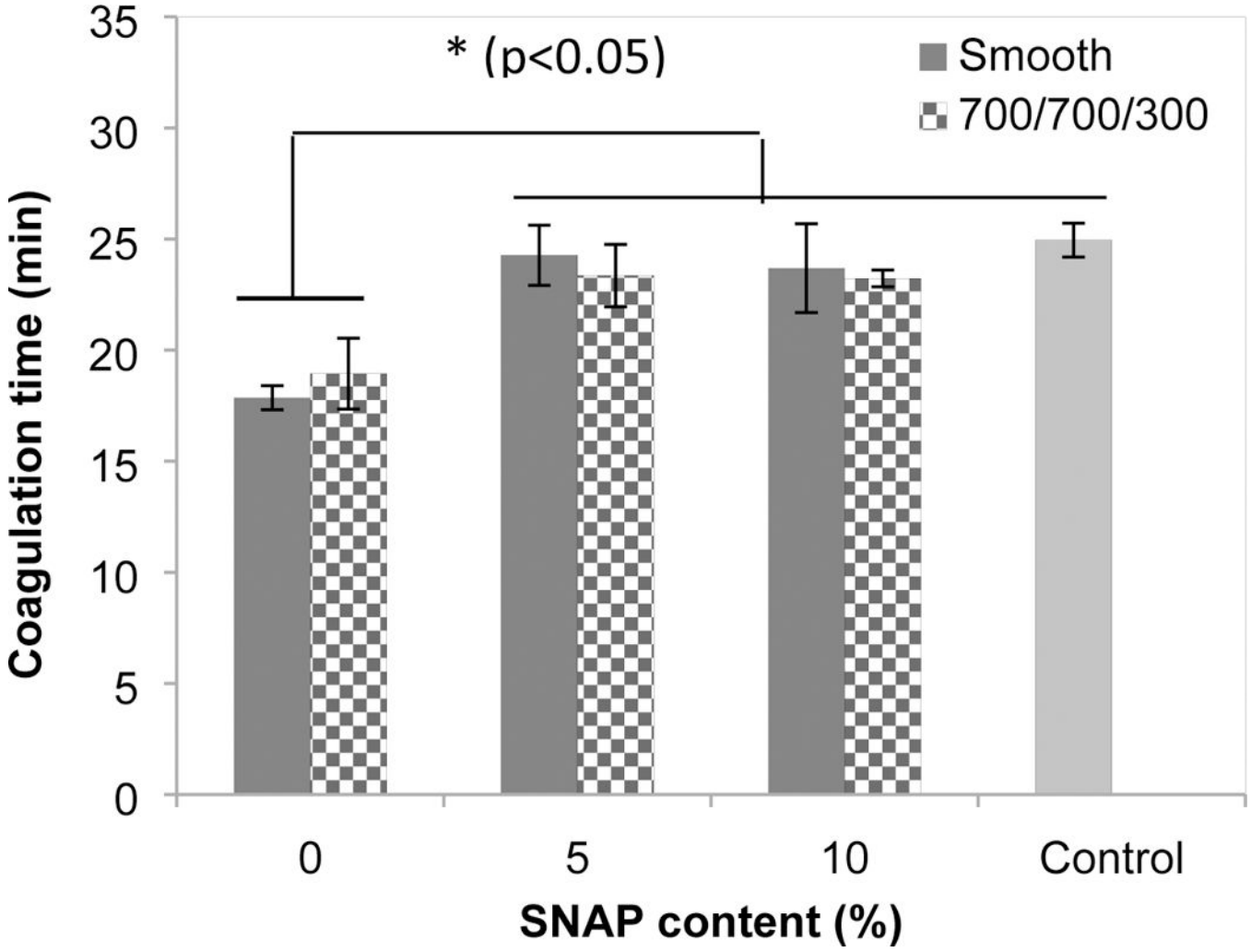

Fig. 1.

Coagulation time of human plasma incubated with polymer films after coagulation initiated by Ca2+. (Control = human plasma without polymers present).

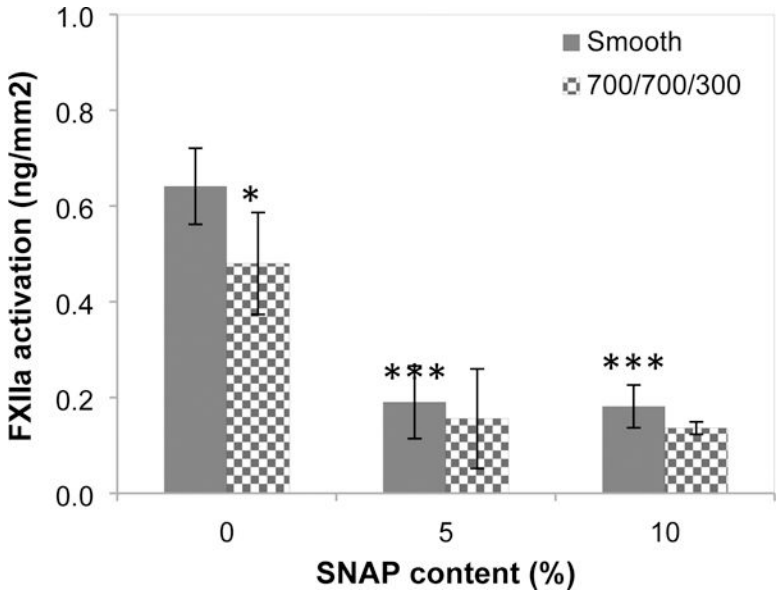

Fig. 2.

FXII contact activation in contact with polymers for 60 min. Statistical analysis was performed to compare the smooth PU films without SNAP. (Statistical symbols, **: $p < 0.01$; ***: $p < 0.001$).

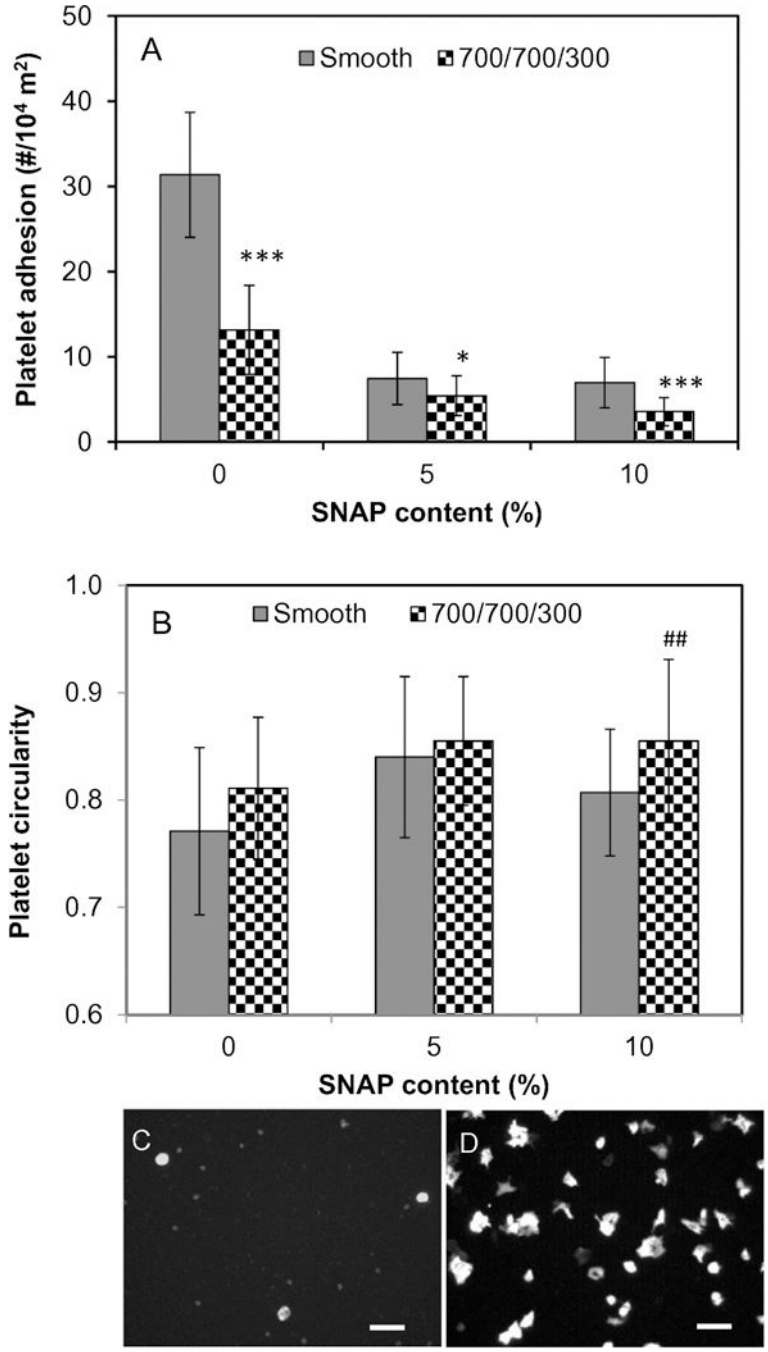

Fig. 3.

Platelet adhesion (A) and activation (B) on polymer surfaces, and representative images of platelets adhered on surface of (C) 10% SNAP impregnated 700/700 nm and (D) smooth PU films without SNAP impregnation, showing different platelet morphologies. Scale bar = 10 μm. Statistical symbol (*) shows the significance compared to the corresponding smooth PU films with same SNAP contents, *: $p < 0.05$; **: $p < 0.01$; ***: $p < 0.001$. Statistical symbol (#) shows the significance compared to the smooth PU film with 0% SNAP, ##: $p < 0.01$; ###: $p < 0.001$).

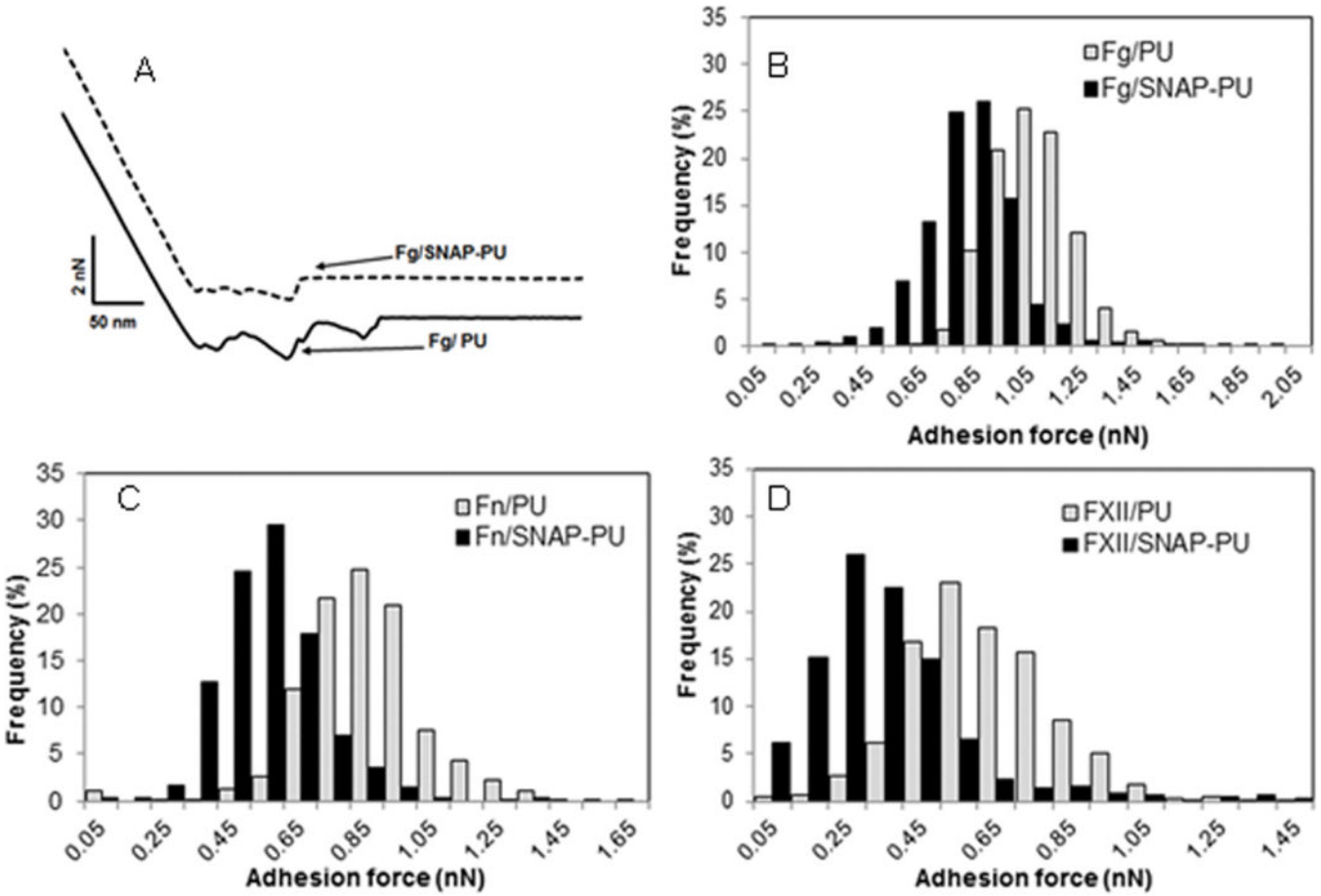

Fig. 4.

Representative adhesion force curves for fibrinogen and polymer film surfaces (A), and adhesion force distribution of proteins and polymer film surfaces for fibrinogen (B), fibronectin (C), and FXII (D) in PBS buffer.

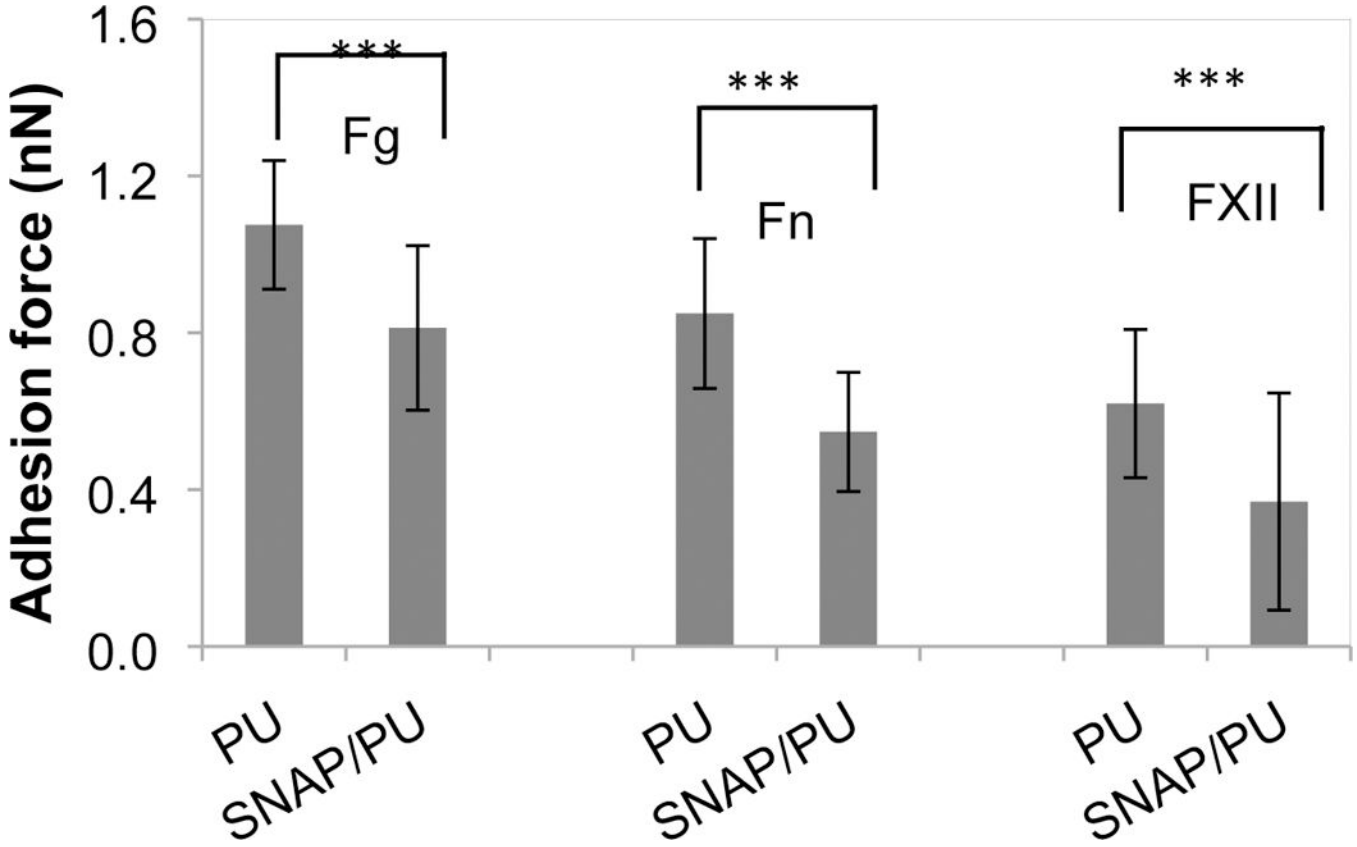

Fig. 5.
Average adhesion forces between protein and polymer surfaces in PBS (***: $p < 0.001$).

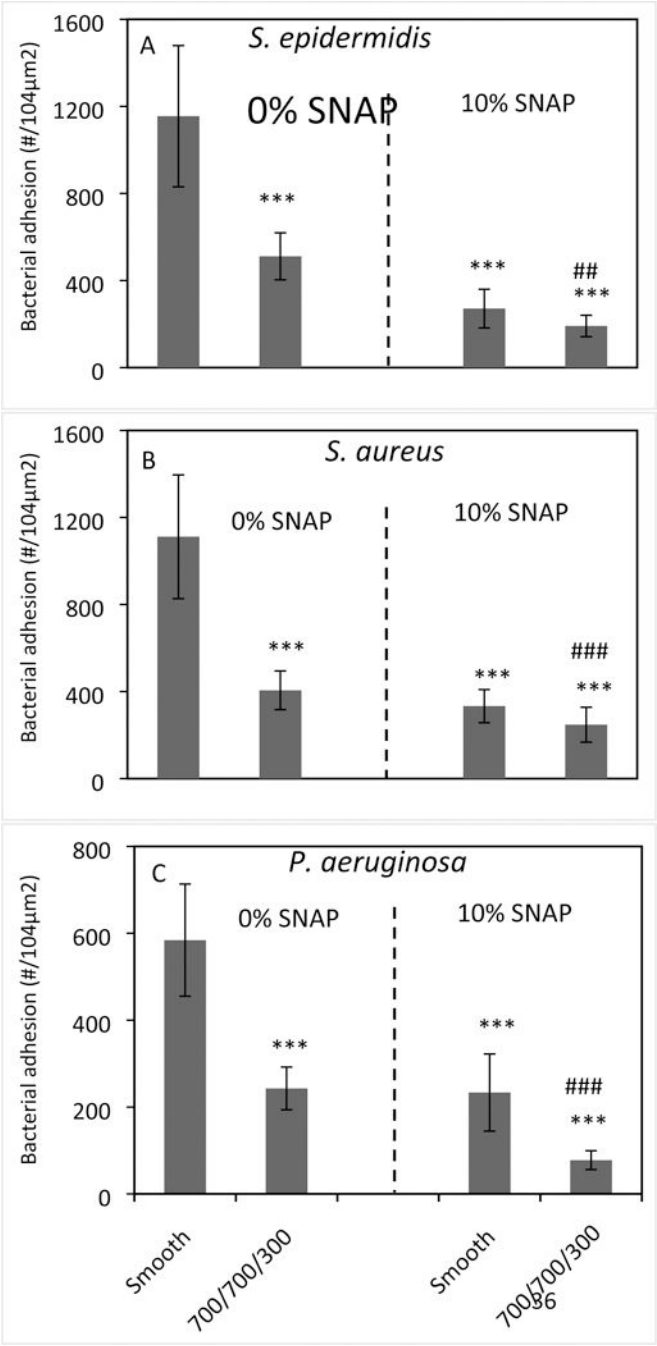

Fig. 6.

Bacterial adhesion on polymer film surfaces in plasma containing (A) S. epidermidis, (B) S. aureus for 2 h and (C) P. aeruginosa for 1 h under static condition. (Statistical analysis, ***: comparing to regular smooth PU with SNAP 0%, $p < 0.001$; ## or ###: comparing to textured PU with SNAP 0% or smooth PU with SNAP 10%, ##: $p<0.01$; ###: $p<0.001$.)

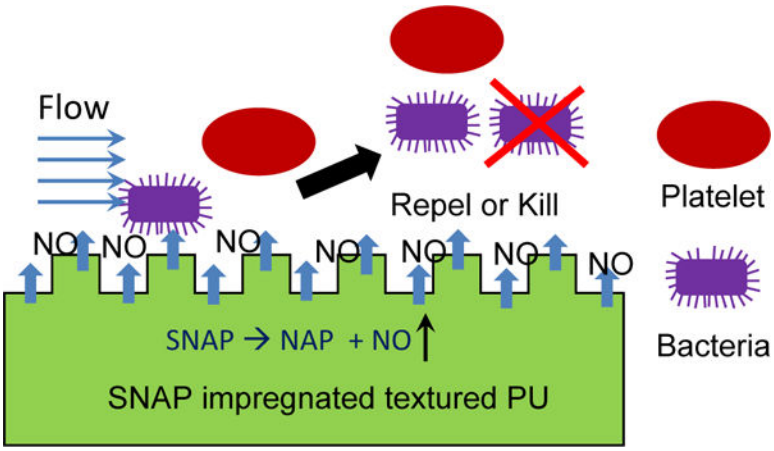

Scheme 1.

Textured polyurethane (PU) is impregnated with SNAP. The combination of surface texturing and NO release mimics the inner surface of blood vessels and inhibits platelet and bacterial adhesion.

Table 1.

Platelet adhesion reduction (%) compared to smooth PU surfaces in plasma under static condition, and statistical analysis of the bacterial adhesion results using two-sample t-test of the mean (p-values)

	Texture only	Smooth (SNAP only)		Texture + SNAP	
	0% SNAP	5% SNAP	10% SNAP	5% SNAP	10% SNAP
Adhesion reduction (%)	58	76	78	83	89
p-value	< 0.001	< 0.001	< 0.001	< 0.001	< 0.001

Table 2.

Bacterial adhesion reduction (%) compared to smooth PU surfaces in plasma under static condition, and statistical analysis of the bacterial adhesion results using two-sample t-test of the mean (p-values)

Surface modification	***S. epidermidis* (%)**	***S. aureus* (%)**	***P. aeruginosa* (%)**
Texturing only	56 ($p < 0.001$)	64 ($p < 0.001$)	58 ($p < 0.001$)
NO release only	76 ($p < 0.001$)	70 ($p < 0.001$)	60 ($p < 0.001$)
Texturing+NO release	84 ($p < 0.001$)	78 ($p < 0.001$)	87 $p < 0.01$)